NAIST-IS-MT9551124

Master's Thesis

Blood Vessel Visualization using a Micromotor Type IVUS

Md. Salimuzzaman

February 14, 1997

Department of Information Processing
Graduate School of Information Science
Nara Institute of Science and Technology

Master's Thesis
submitted to Graduate School of Information Science,
Nara Institute of Science and Technology
in partial fulfillment of the requirements for the degree of
MASTER of ENGINEERING

Md. Salimuzzaman

Supervisors: Kunihiro Chihara, Professor
Kiyohiro Shikano, Professor
Osamu Oshiro, Associate Professor

Blood Vessel Visualization using a Micromotor Type IVUS*

Md. Salimuzzaman

Abstract

The objective of the present study is to develop a new intravascular ultrasound (IVUS) endoscope using a micromotor, in which ultrasound beam is scanned radially by a micromotor instead of a rotation transmitting wire. In this micromotor type IVUS endoscope, a micromotor attached with an ultrasound reflecting mirror and an ultrasound transducer are inserted in a catheter. The rotation of the micromotor is performed and controlled by an external magnetic field. This micromotor type IVUS endoscope was applied to observe the inside of blood vessels through in vitro experiments. The preliminary results suggested that a micromotor type IVUS has sufficient ability to define the blood vessel morphology precisely and can solve the problems of conventional IVUS endoscopes.

Keywords:

IVUS, micromotor type IVUS, catheter, B-mode imaging, ultrasound diagnosis, blood vessel visualization, in vitro experiment

*Master's Thesis, Department of Information Processing, Graduate School of Information Science, Nara Institute of Science and Technology, NAIST-IS-MT9551124, February 14, 1997.

マイクロモータ型超音波血管内視鏡を用いた血管内可視化方法*

モハマド サリム ッザマン

内容梗概

近年、超音波血管内視鏡を用いて血管内可視化の研究が盛んに行われ、血管病変の診断が可能となってきた。これらの研究で用いられている超音波血管内視鏡に焦点を当ててみると、従来は体外モータにつながるワイヤを介した超音波内視鏡を血管内腔に挿入して目的の部位近傍に到達させ、その血管及び血管周辺の観察を行ってきた。従来方法では、ワイヤを用いるため、超音波血管内視鏡の振動、超音波ビーム走査の不安定、ワイヤの破損などを引き起こす危険性が指摘され、これらは効果的な治療の妨げになっている。本研究では、このような問題を解決するためマイクロモータ型超音波血管内視鏡を提案した。ここで用いた超音波血管内視鏡では、血管内にマイクロモータ駆動系を持つ超音波カテーテルプローブを挿入し超音波走査を行い、マイクロモータの回転は外部磁界によって行うものであった。本論文では、このマイクロモータ型超音波血管内視鏡を用い、血管内の観察を行った。実験結果より、マイクロモータ型超音波血管内視鏡が実装可能であることを示した。

キーワード

超音波血管内視鏡, マイクロモータ型超音波血管内視鏡, カテーテル, B-モード表示, 超音波診断, 血管内可視化, 生体外実験

*奈良先端科学技術大学院大学 情報科学研究科 情報処理学専攻 修士論文, NAIST-IS-MT9551124, 1997 年 2 月 14 日.

Contents

Introduction **1**

1 Ultrasound **3**

1.1. Ultrasound medicine 3

1.2. Displaying modes for pulse-echo method 5

2 Intravascular Ultrasound(IVUS) Imaging **12**

2.1. IVUS endoscopy 12

2.2. Conventional IVUS scanning methods 14

2.3. Assessment of conventional IVUS methods 16

3 Micromotor Type IVUS **19**

3.1. Concept of a micromotor type IVUS 19

3.2. Characteristics of permanent magnet rotation 21

3.3. Catheter 23

4 Measurement System **25**

4.1. External magnetic field 25

4.2. Signal acquisition system 27

4.3. Image reconstruction process 31

5 Experiments and Results **33**

5.1. Phantom experiments 33

5.2. In vitro experiments 41

6 Discussion **46**

Conclusions **48**

Acknowledgements **49**

References **50**

List of Figures

1.1 A-mode display 6
1.2 B-mode display 7
1.3 B-mode image 8
1.4 Mechanical scanning probe 9
1.5 Electronically scanned linear array probe 10
1.6 Compound scanning probe 11

2.1 An IVUS inserted into a blood vessel for diagnosing the blood vessel stricture 13
2.2 Transducer rotating method 14
2.3 Mirror rotating method 15
2.4 Electronical scanning method 16
2.5 Demerits of the mechanical scanning IVUS, (a)vibration on the wire, (b)trouble of wire 17

3.1 A micromotor type IVUS endoscope, (a)schematic view of the magnet and the mirror, (b)photograph of the magnet attached with a mirror 20
3.2 Characteristics of the permanent magnet rotation 22
3.3 Catheter for a micromotor type IVUS endoscope, (a)schematic view of the catheter, (b)photograph of the catheter used for experiments 24

4.1 Generation of external magnetic field 26
4.2 Block diagram of the data acquisition system 27

4.3 Signal acquisition system, (a)Digital storage oscilloscope, (b)Host computer 29
4.4 Frequency response of a Bessel band-pass filter 30
4.5 Graphical workstation 31
4.6 Image reconstruction process 32

5.1 A view of phantom experiment 34
5.2 A photograph of phantom1 35
5.3 Results of phantom1, (a)an echo signal, (b)reconstructed image. . 36
5.4 A photograph of phantom2 37
5.5 Results of phantom2, (a)an echo signal, (b)reconstructed image. . 38
5.6 A photograph of phantom3 39
5.7 Results of phantom3, (a)an echo signal, (b)reconstructed image. . 40
5.8 A view of in vitro experiment 41
5.9 A photograph of arterial specimen1 42
5.10 Results of arterial specimen1, (a)example of an echo signal, (b)cross-sectional image of arterial specimen1. 43
5.11 A photograph of arterial specimen2 44
5.12 Results of arterial specimen2, (a)example of an echo signal, (b)cross-sectional image of arterial specimen2. 45

List of Tables

2.1 Comparison of the both scanning methods 18

Introduction

Ultrasound is defined as sound not used for human hearing purposes[1]. During the second world war, it was commonly used in the battleground for detecting susceptible metals inside the ground. One of the important features of any ultrasound instrumentation system is a transducer which was invented by P.Langevin in the beginning of 20th century. This transducer is typically incorporated with a piezoelectric element, which converts electrical signals into mechanical vibrations and vice versa[2].

In 1942, K. T. Dussik first introduced the possibility of ultrasound in medical field[3], and in 1949 he applied ultrasound technology to diagnose cerebral diseases[4]. In the beginning of ultrasound diagnosis history, the A mode or amplitude mode was commonly used, in which only the echo amplitude could be displayed as a function of depth of penetration. In 1953, J. J. Wild introduced the two-dimensional echogram[5] in which he scanned the ultrasound transducer over a region of an organ. This method is called B-mode imaging which is most commonly used in today's ultrasound diagnosis.

The ultrasound diagnosis has become a pivotal and widely accepted means for the noninvasive imaging of human body in various medical fields; obstetrics, gynecology, abdomen, cardiology and so on, and it also become possible to visualize the moving structures inside a human body on real-time. Several ten years ago, ultrasound diagnosis was performed only at the surface of a human body. The size of an ultrasound transducer was not small enough to place it closer to some internal organs of a human body; prostate, uterus, ovary and blood vessel. Inaccessibility of ultrasound with the obscure by gas or bone was also a problem to visualize the inside of these organs.

During the last decade, an ultrasound transducer has been smaller and it be-

came possible to develop an ultrasound endoscope to observe the internal organs of a human body from a very close position[6]. In an ultrasound endoscope, an ultrasound transducer with a resonant frequency higher than 10MHz is mounted on the tip of a catheter which is inserted inside a human body. In recent ultrasound diagnosis, an ultrasound endoscope plays an important role to provide information concerning the prostate and the rectal wall from rectum, the uterus and the ovaries from vagina, the bladder wall from bladder, and the stomach wall from stomach[7]. The ultrasound endoscope that deals with the non-invasive testing of vascular diseases is called intravascular ultrasound (IVUS) endoscope. The IVUS endoscope is commonly used to observe the blood vessel morphology, to diagnose blood vessel diseases like vessel stricture and vessel lesion, to detect the plaque location inside a blood vessel and to measure the plaque thickness[8, 9, 10, 11].

In most conventional IVUS endoscope, a cross-sectional image of a blood vessel is obtained by scanning ultrasound beam radially[12, 13]. In this method, the radial scanning of an ultrasound beam is performed by a mechanical motor located at the outside of a human body. This mechanical motor is connected with an ultrasound reflecting mirror inside a catheter through a rotation transmitting wire. One of the disadvantage of a conventional IVUS endoscope is the mechanical vibration which transmits through the rotation transmitting wire[14, 15]. This disadvantage is caused by the rotation of the mechanical motor and it results in wrench and snap of the rotation transmitting wire and harmful to a blood vessel. Furthermore, the images reconstructed with this conventional IVUS endoscope can not correspond to the accurate structure of a blood vessel due to the unstable rotation of the ultrasound reflecting mirror.

To solve the above problems, I have developed a new IVUS endoscope using a micromotor instead of a mechanical motor and a rotation transmitting wire[16]. To evaluate the measurement accuracy of this micromotor type IVUS endoscope, I have performed several phantom experiments and applied this micromotor type IVUS endoscope to observe the inside of blood vessels through in vitro experiments.

Chapter 1

Ultrasound

1.1. Ultrasound medicine

In ultrasound diagnosis, an ultrasound transducer is used to transmit/receive ultrasound beam, and an ultrasound image is reconstructed from the reflected wave(echo), which is called echo method. Ultrasound beam from a transducer is reflected at the border between two media having a different acoustical impedance. The reflected signals are received by the same transducer. The distance between the transducer and the border is calculated by multiplying the velocity of ultrasound inside the media with the half time of ultrasound flight. In echo method, there are pulsed wave technique and continuous wave technique. All conventional medical ultrasound imaging systems are based on the pulse wave technique which is called pulse-echo method. By moving a transducer over a body region or by using an array of such transducers, a cross-sectional image can be formed.

Ultrasound is also a radiation like X-ray and laser light, but there are some marked differences between ultrasound and both X-ray and light. Ultrasound waves propagate so slowly that transit time can be measured easily for the distances traveled in a human body. Conversely, the propagation speed is fast enough to gather all of the data needed for a cross-sectional image and to view a moving object. Because the size of an ultrasound imaging device is small enough for moving from one place to another, a patient does not need to move from the bed for a checkup. Furthermore, the internal structure of an ultrasound transducer is very simple and the production cost of an ultrasound diagnosis system is not

very expensive comparing with other medical imaging systems like X-ray, CT scan and MRI.

Several studies in various clinical fields have shown ultrasound to be an accurate and versatile technique yielding a cross-sectional image with a high resolution. Some common uses of ultrasound diagnosis are mentioned below[7],

- Obstetrics
  Ultrasound plays a major role in management of both normal and complicated pregnancies. The common uses are;
  - to monitor development of the fetus,
  - to diagnose maternal and foetal disorders.
- Gynecology
  In comparison with obstetrics, the use of ultrasound in gynecology is more limited. The most common applications are;
  - the size and shape assessment of uterus and cervix,
  - diagnosis and follow-up of malignant tumors of uterus,
  - detection of ovarian cysts.
- Abdomen
  Ultrasound imaging is used for;
  - assessment of liver size and shape,
  - detection of gall stones and inflammation of the gall bladder,
  - diagnosis of pancreatic carcinoma,
  - management of spleen trauma.
- Cardiovascular System
  Ultrasound plays a pivotal role in;
  - diagnosis of valve disorders,
  - assessment of ventricle function,
  - diagnosis of pericardial effusion,

- evaluation of congenital heart diseases,
- diagnostic of cardiac tumors.

This section shows that the most important features of ultrasound modality are, first, its ability to produce images of moving structures, second, its portability and, third, its low cost[17]. These merits have made ultrasound the most widely accepted means for the noninvasive imaging of a human body comparing with other medical imaging systems.

1.2. Displaying modes for pulse-echo method

All conventional medical ultrasound imaging systems are based on a pulse-echo method utilizing backscattered echo waves. Pulse-echo methods can be classified into A-mode, B-mode, M-mode and, C-mode depending on its displaying method[18]. Here I will explain only the A-mode and B-mode.

- A or Amplitude Mode

  A-mode is a one-dimensional display of echo amplitude as a function of distance of penetration, which is equal to ct/2, where t is the time of flight of pulse and c is the velocity of ultrasound in the media. Fig.1.1 illustrates this display method. This is used in eye examinations, where precise measurement of axial length of the eye is required.

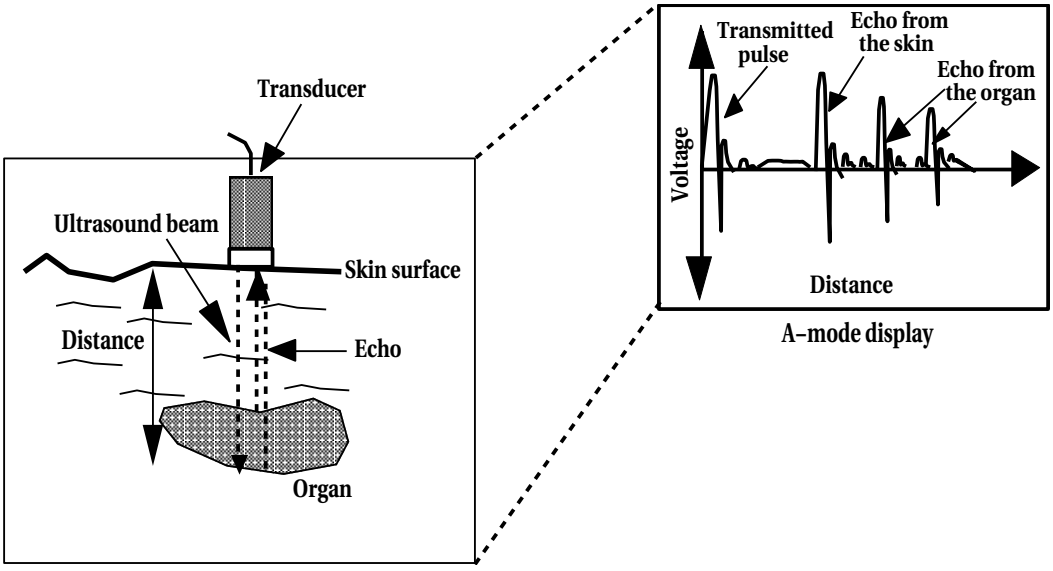

Figure 1.1. A-mode display

- B or Brightness Mode

  Fig.1.2 shows the B-mode display. In a B-mode, the amplitude of the echo signals are displayed as the electron beam intensity of a cathode ray tube(CRT). This method is commonly used in various sort of clinical purposes.

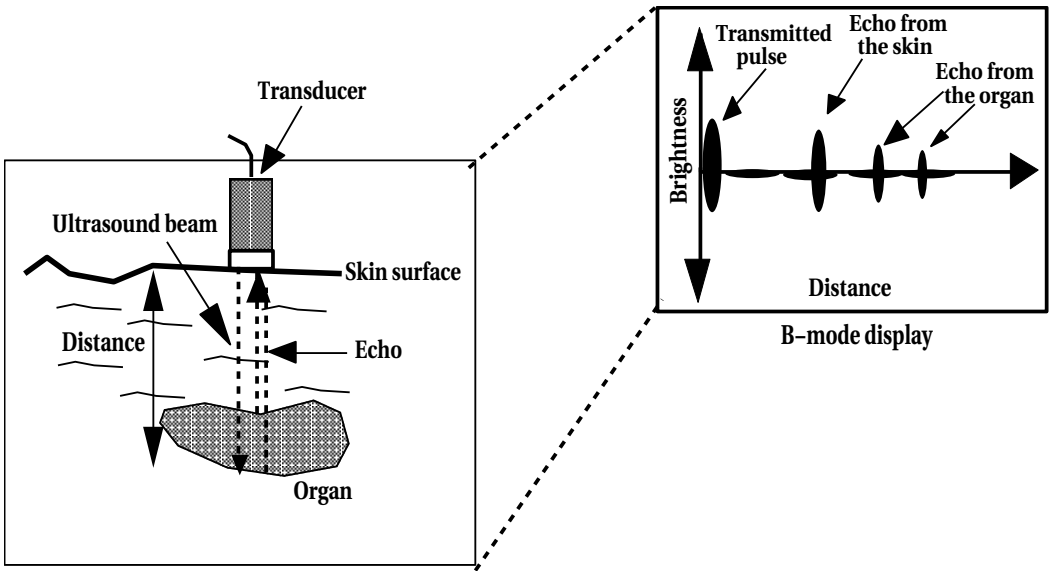

Figure 1.2. B-mode display

In a B-mode, the cross-sectional image of an organ can be built up by scanning an ultrasound transducer over the region of an organ. Fig.1.3 illustrates a B-mode image. The scanning of the ultrasound transducer can be performed by manually or automatically. The disadvantages of a manual B-mode scanner are that it depends on the operator skill to obtain desired images and that it takes much time comparing with an automatic scanner.

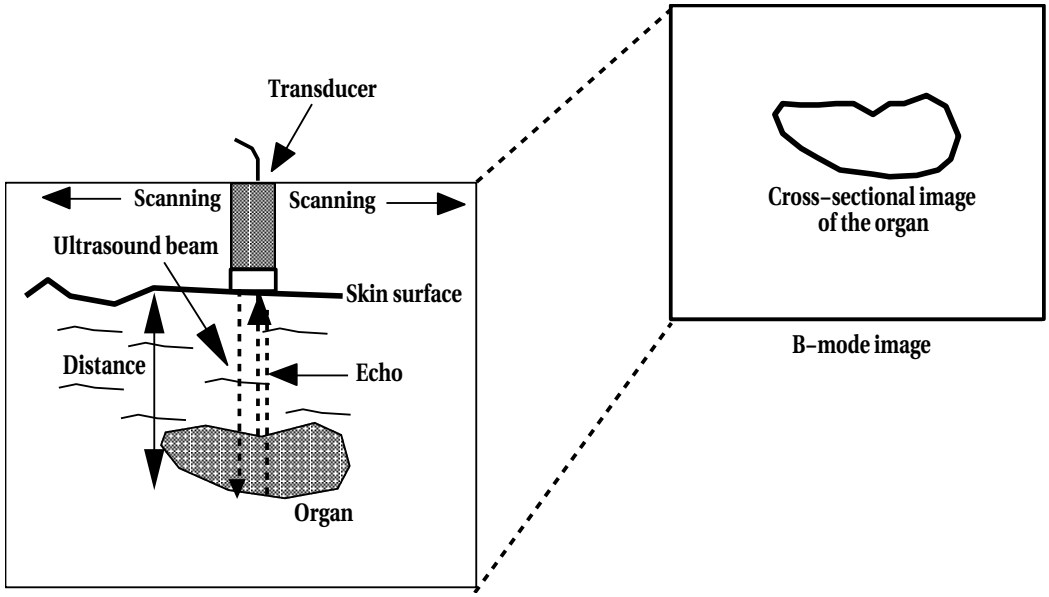

Figure 1.3. B-mode image

The methods for an automatic scanning can be classified into mechanical scanning method, electronical scanning method and compound scanning method.

- Mechanical scanning method
  Fig.1.4 illustrates mechanical scanning method. In a mechanical scanning method, an ultrasound transducer is rocked back and forth by a mechanical motor. Each sweep of the transducer produces one image. However, the oscillation of the scanner against skin may be uncomfortable for the patient and this motion causes the images to be blurred, since the tissues may moved by vibration, and it takes much time to reconstruct a single cross-sectional image. The advantage of a mechanical scanning as compared with an electronical scanning is that the internal structure and electronic circuit are very simple.

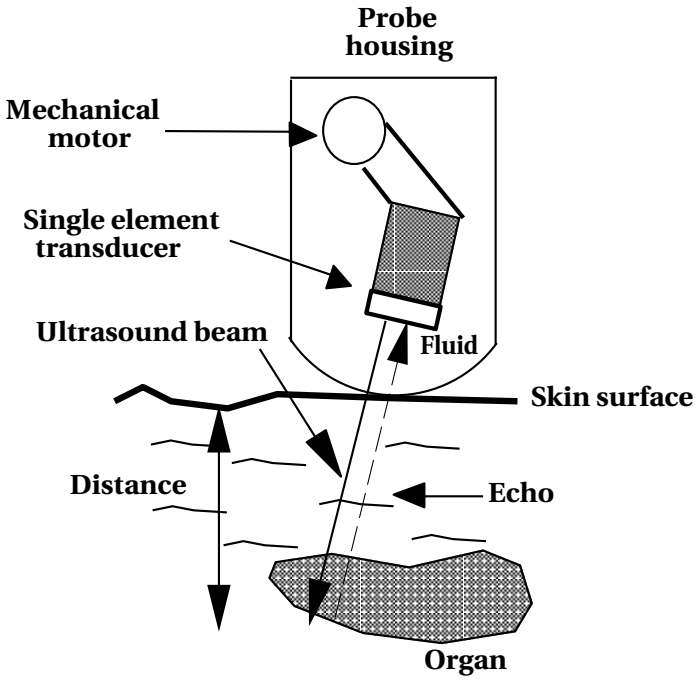

Figure 1.4. Mechanical scanning probe

– Electronical scanning method

There are three different types of electronical scanning methods; the linear array, the linear phased array, and the annual array. Here I will explain only about the linear array. Fig.1.5 illustrates a typical linear array system. In a linear array, the ultrasound probe consists of several transducers in an array structure. The transmission/reception of the ultrasound beam at each transducer is carried out sequentially. The switching circuit controls this sequence. The disadvantage of a linear array is its high production cost.

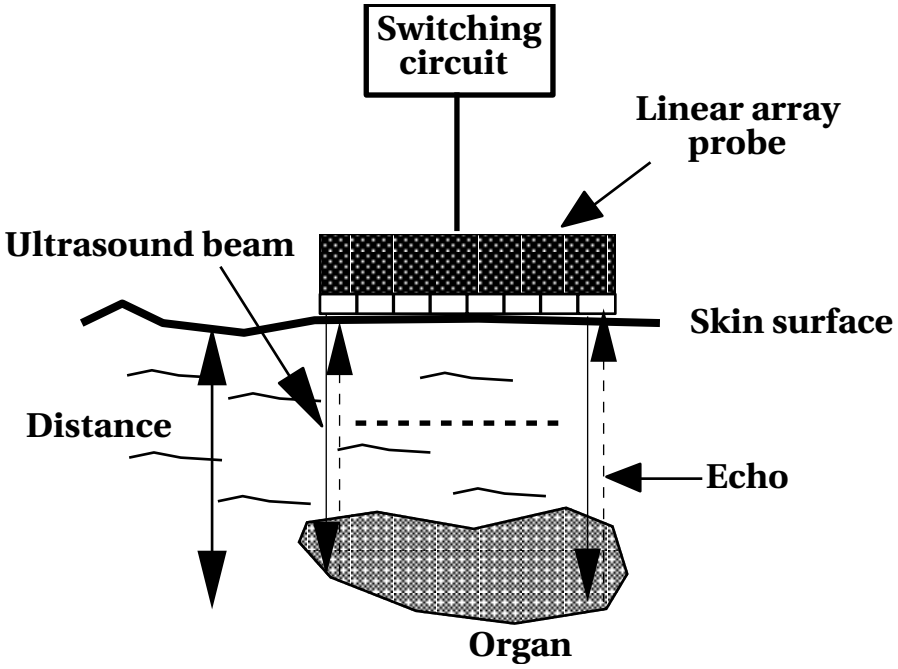

Figure 1.5. Electronically scanned linear array probe

– Compound scanning method

To obtain a three-dimensional image of a target by using the conventional mechanical scanning method, it takes a very long time. On the other hand, for electronical scanning method it is needed to construct a probe consists of transducers in a two-dimensional array structure which may make the internal structure more complicated. To solve these problems, the compound scanning method was developed. Fig.1.6 illustrates the compound scanning method consisting of the previous two scanning methods. This scanning method can provide a three-dimensional image of a target. Here an linear array probe is used to obtain a cross-sectional image and it is moved on the X-axis by a mechanical motor. From these cross-sectional images, the three-dimensional image of a target is reconstructed.

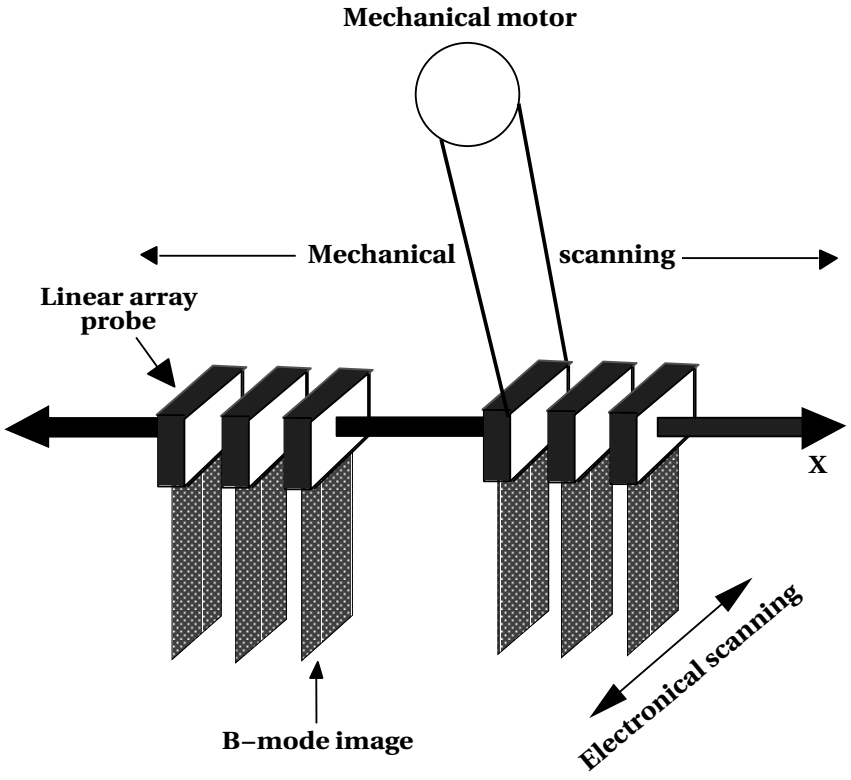

Figure 1.6. Compound scanning probe

Chapter 2

Intravascular Ultrasound(IVUS) Imaging

2.1. IVUS endoscopy

The previous chapter showed the conventional ultrasound imaging methods, in which the ultrasound scanning was performed on the surface of a human body. In these methods, it is not possible to place the ultrasound transducer closer to the organ of interest. These systems also do not permit, in some cases, the proper image reconstruction of some organs because of the obscure by gas or bone. To solve these problems, the ultrasound endoscopes were developed. Nowadays, this is one of the attracting research topics among the ultrasound researchers.

The ultrasound endoscope that deals with vascular diseases is called intravascular ultrasound (IVUS) endoscope. In IVUS endoscope, an ultrasound transducer with a resonant frequency higher than 10 MHz is mounted on the tip of a catheter which is inserted inside a human body for visualizing a blood vessel lumen and the surroundings. The ultrasound transmission is performed radially to observe the cross-section of the target. Example of applications are the imaging of a blood vessel stricture at the pre stage of atherosclerosis, blood vessel lesion, etc. Fig.2.1 illustrates diagnosis of the blood vessel stricture.

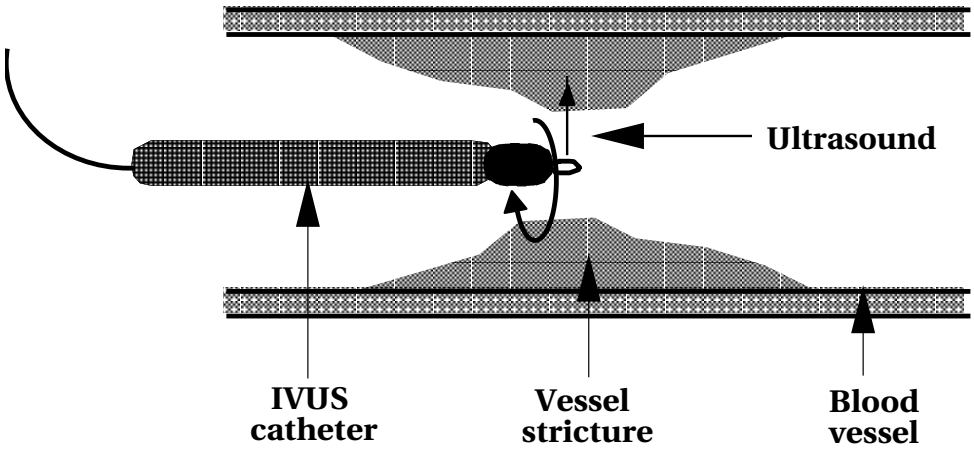

Figure 2.1. An IVUS inserted into a blood vessel for diagnosing the blood vessel stricture

2.2. Conventional IVUS scanning methods

The scanning methods for IVUS can be classified into mechanical scanning method and electronical scanning method. For both of these methods, a guide wire is necessary for the catheter to guide the way inside a blood vessel.

- Mechanical scanning method
  In the mechanical scanning method, the radial scanning of the ultrasound is performed by a mechanical motor located at the outside of a human body. The motor is connected with the catheter through a wire. There are several types of mechanical scanning catheters available in the market.

  – Transducer rotating method
    Fig.2.2 illustrates a mechanical scanning catheter in which the transducer is rotated by the mechanical motor located at the outside of a human body. Here, the direction of the transmitted ultrasound beam is perpendicular to the catheter. This method, in some cases, is influenced strongly by near-field as the distance between the transducer and the target is very small[19].

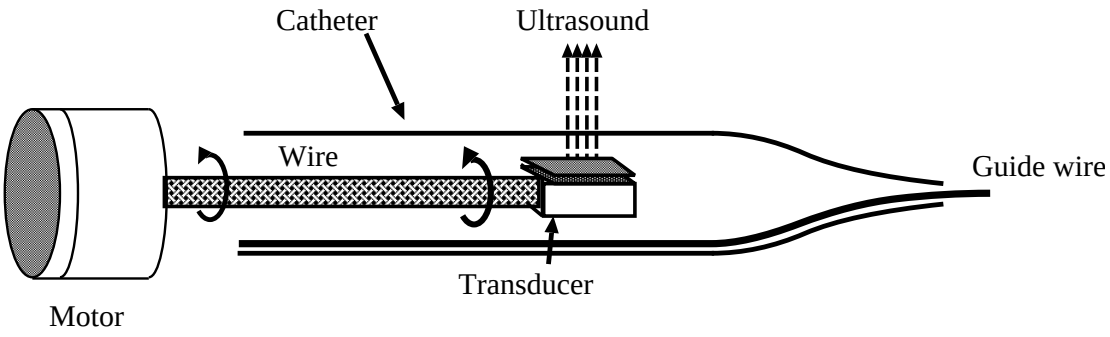

Figure 2.2. Transducer rotating method

– Mirror rotating method

  Fig.2.3 illustrates another mechanical scanning catheter. Here an ultrasound reflecting mirror is also inserted into the catheter. The ultrasound beam from the transducer is transmitted towards the target reflected by the mirror. In the same way, the echo signals from the target is reflected by the mirror and received by the same transducer. The rotation of the mirror is performed and controlled by a mechanical motor located at the outside of a human body. In this method, the influence of near-field is lesser than the transducer rotating method as the distance between the transducer and the target is larger.

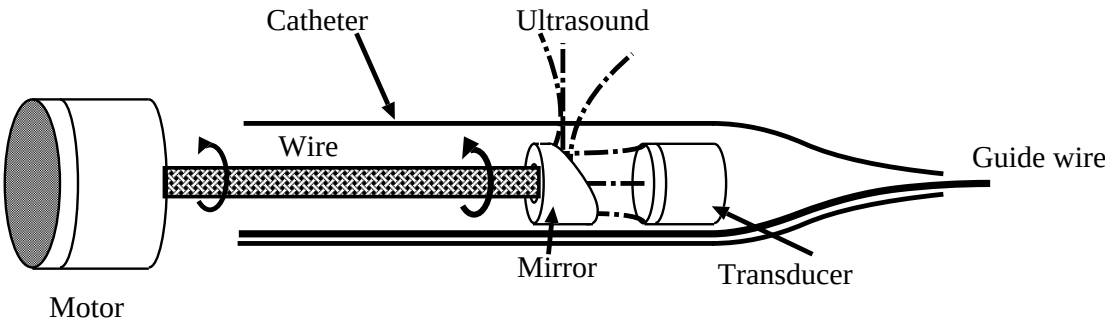

Figure 2.3. Mirror rotating method

- Electronical scanning method
  Fig.2.4 illustrates electronical scanning catheter, where several tiny transducers are arranged in a ring-array structure on the side wall of the catheter and the transmission/reception of the ultrasound beam at each transducer is carried out sequentially. The direction of the transmitted ultrasound beam is perpendicular to the catheter.

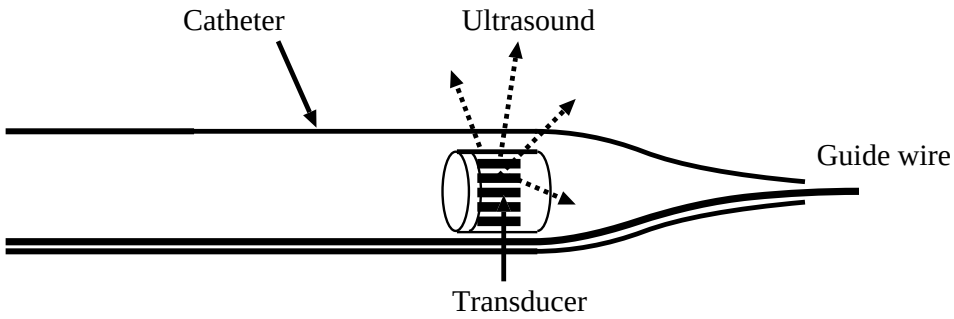

Figure 2.4. Electronical scanning method

2.3. Assessment of conventional IVUS methods

Comparing with the electronical scanning method, the merits of the mechanical scanning method are;

- a number of scan lines can be obtained easily,
- internal structure is simple,
- the caliber of the transducer is larger,
- image resolution is high.

One of the disadvantage of mechanical scanning method is the vibration caused by the rotation of the mechanical motor and it results in wrench and snap of the rotation transmitting wire and harmful to a blood vessel as shown in fig.2.5. Furthermore, the images reconstructed with this system can not correspond to the accurate structures of the target due to this vibration[20]. Comparing with a mechanical scanning method, the merits of the electronical scanning method is that it does not require any scanning wire to perform the radial scan, as a result, it does not suffer from the trouble of vibration, wrench and snap of the wire.

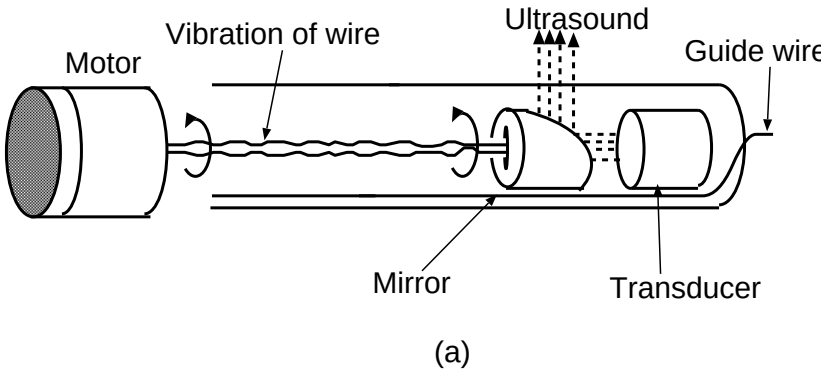

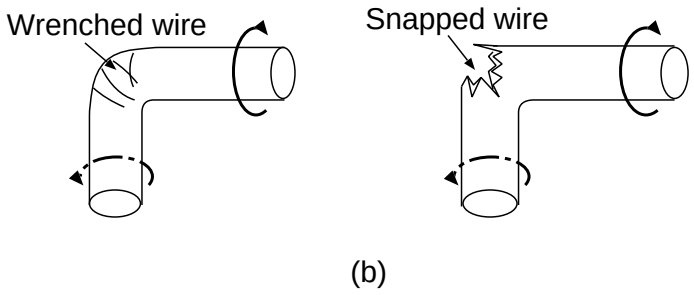

Figure 2.5. Demerits of the mechanical scanning IVUS, (a)vibration on the wire, (b)trouble of wire

Table2.1 summarizes the merits and demerits of the both scanning methods.

Table 2.1. Comparison of the both scanning methods

	Mechanical scanning	Electronical scanning
Internal structure	simple	complicated
Scanning wire	necessary	not necessary
Scan line	numerous	a few
Caliber of transducer	large	small
Resolution	high	low

This table shows the need of a new scanning method for the IVUS endoscope, in which the scanning method is the same as the mechanical scanning method but the scanning wire is not necessary as the electronical scanning method. To fulfill this requirement, I have developed a new IVUS endoscope using a micromotor. The details of this system will be described in the next chapter.

Chapter 3

Micromotor Type IVUS

3.1. Concept of a micromotor type IVUS

In a micromotor type IVUS endoscope, a magnet, an ultrasound reflecting mirror and an ultrasound transducer are inserted into a catheter. The magnet having two poles can be rotated by an external sinuous magnetic field. The rotation can be controlled by the same external magnetic field. As shown in fig.3.1(a), a $SmCo$ permanent magnet is used as a micromotor which is cylinder-shaped and has a diameter of 1mm and a length of 3mm. On the tip of the micromotor, an oval-shaped Al ultrasound reflecting mirror which has a taper angle of 45deg and a diameter of 1mm is attached. Ultrasound beam from the transducer is reflected by the mirror and moves toward the target. Similarly, the echo signals from the targets are reflected by the mirror and received by the same transducer. The rotation of the magnet is performed by the external magnetic field generated by a coil. Fig.3.1(b) shows a photograph of the permanent magnet attached with the mirror.

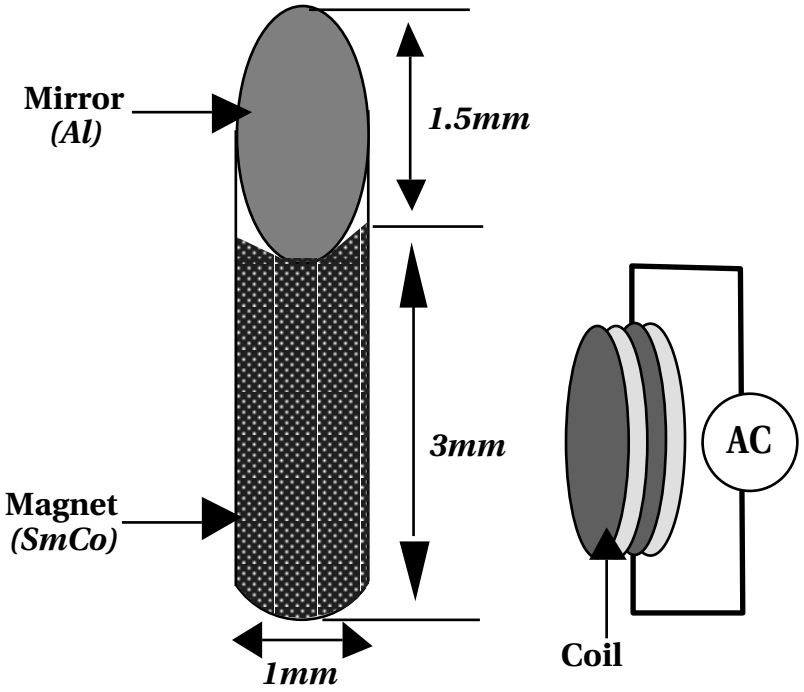

(a)

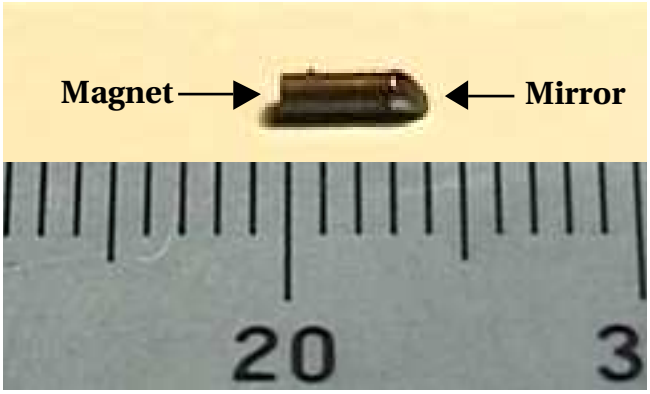

(b)

Figure 3.1. A micromotor type IVUS endoscope, (a)schematic view of the magnet and the mirror, (b)photograph of the magnet attached with a mirror

3.2. Characteristics of permanent magnet rotation

The rotation frequency of the micromotor is proportional to the frequency of the external magnetic field[21]. The characteristics of the permanent magnet rotation in respect to the magnitude of the external magnetic field are;

- Fig.3.2(a) shows the characteristics of the permanent magnet rotation in a magnitude B of 0.01mT. The magnet does not rotate at the frequency of the external magnetic field is below 20Hz and the magnet rotates unstably at the frequency range of the external magnetic field between 20-70Hz.
- Fig.3.2(b) shows the characteristics in a magnitude of 0.02mT. The magnet rotates stably at the frequency range between 30-80 Hz.
- Fig.3.2(c) shows the characteristics in a magnitude of 0.025mT. The magnet rotates stably at the frequency range between 30-80Hz.
- Fig.3.2(d) shows the characteristics in a magnitude of 0.03mT. The magnet rotates stably at the frequency range between 25-115Hz.

The frequency range of the micromotor rotation increases in proportional to the magnitude of the external magnetic field.

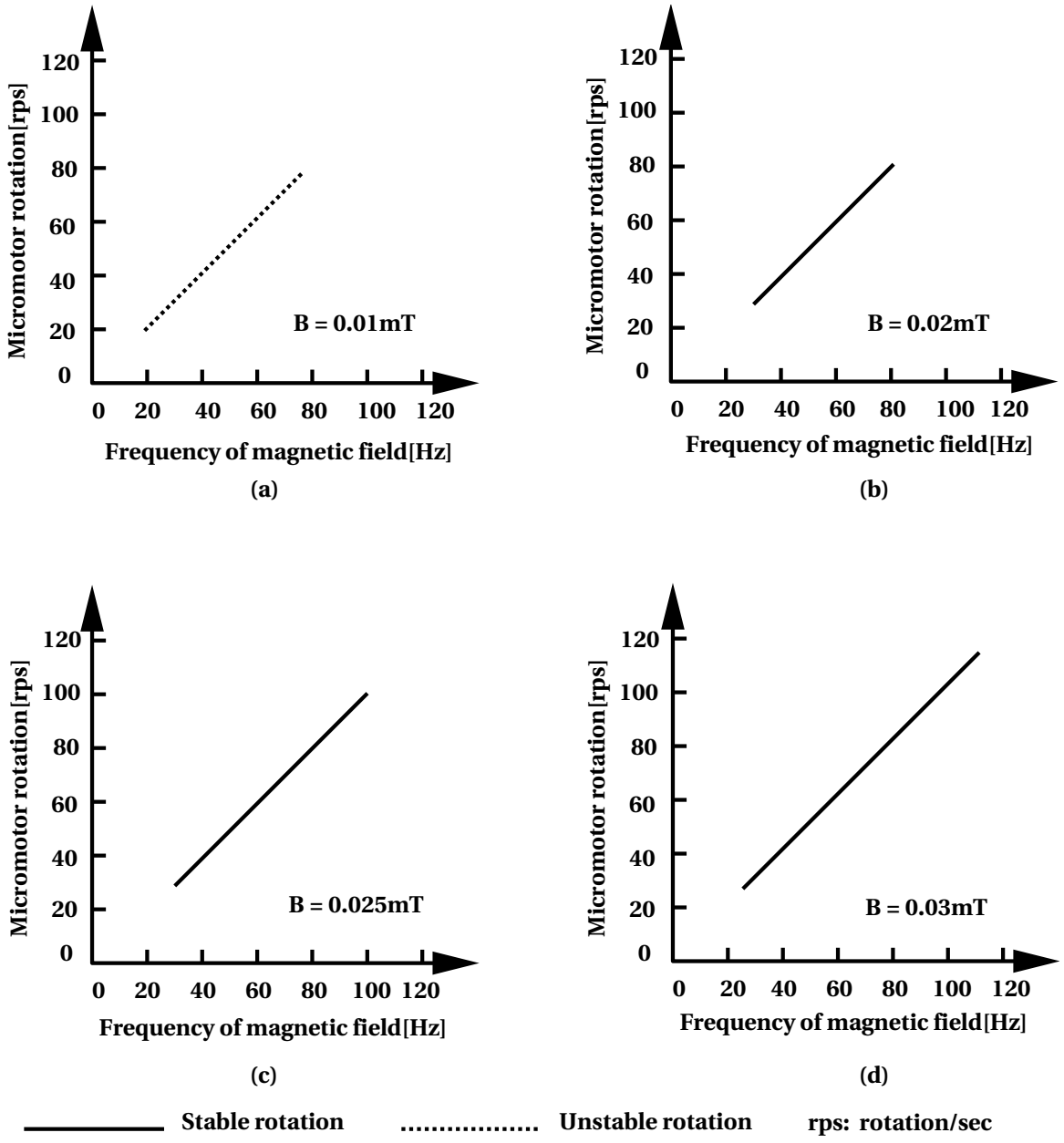

Figure 3.2. Characteristics of the permanent magnet rotation

3.3. Catheter

I have developed a catheter for micromotor type IVUS endoscope[22]. Fig.3.3(a) shows the schematic view of this catheter. An ultrasound transducer having a diameter of 1.2mm and a resonant frequency of 20MHz is used to transmit and receive ultrasound beam. The magnet attached with the ultrasound reflecting mirror and the ultrasound transducer are mounted in a tube. The distance between the ultrasound reflecting mirror and the ultrasound transducer is set at 3mm.

Fig.3.3(b) shows a photograph of the catheter for the experiments. Here the micromotor is mounted on a shaft of 1.4mm diameter for smooth rotation around the axis. A tube made of Tecoflex with a inner diameter of 1.5mm and a outer diameter of 1.9mm is used as the catheter tube. As the outer diameter of the catheter is 1.9mm, it has the ability to be inserted easily into a human arterial lumen with a diameter of 3mm.

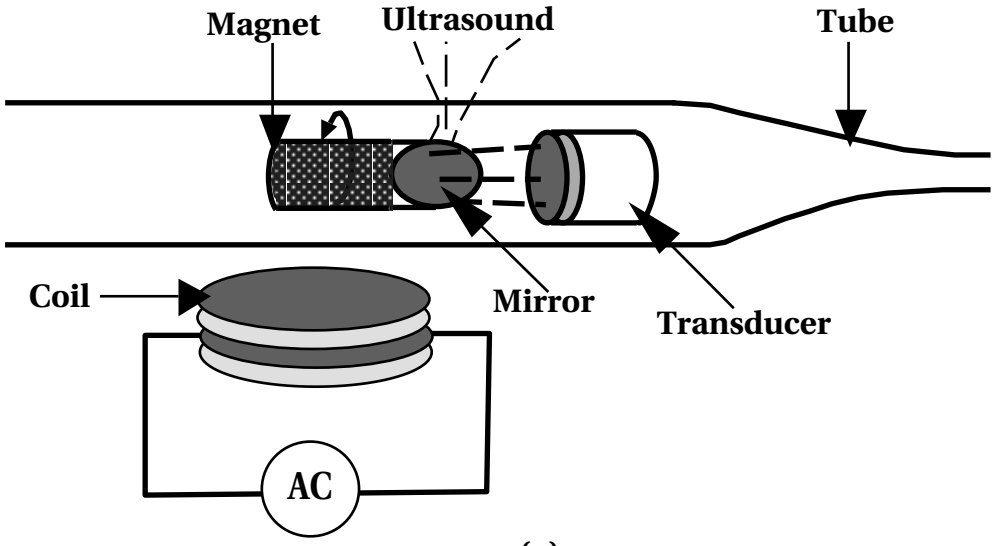

(a)

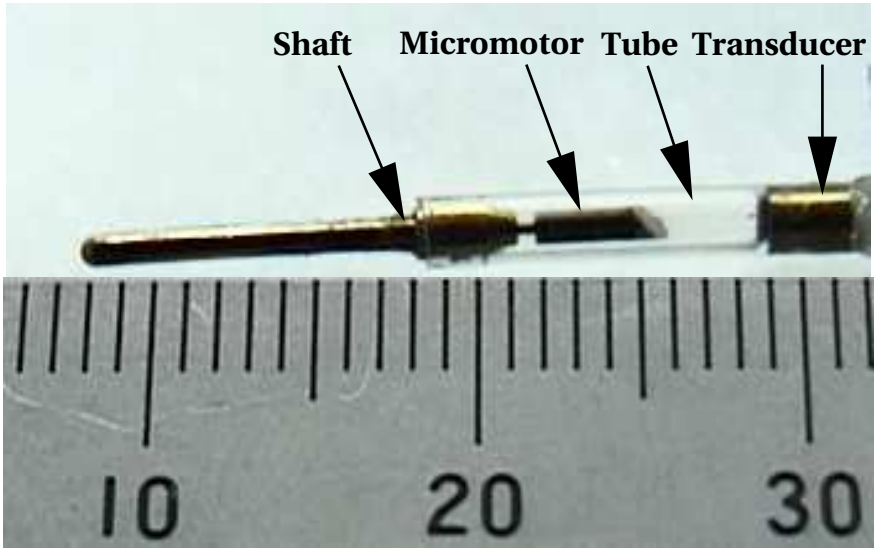

(b)

Figure 3.3. Catheter for a micromotor type IVUS endoscope, (a)schematic view of the catheter, (b)photograph of the catheter used for experiments

Chapter 4

Measurement System

4.1. External magnetic field

In a micromotor type IVUS endoscope, the permanent magnet can be rotated by an external sinuous magnetic field and the rotation frequency can be controlled by the frequency of the external magnetic field. In present system, this external magnetic field is generated from a coil. Fig.4.1 shows a photograph of the coil connected with a slidac. The coil is connected with a slidac for generating a strong magnetic field. As a result, it became possible to place the catheter at a suitable distance from the coil center. The slidac of present system can generate an alternating current of 3A max, which corresponds to a magnitude of 0.03mT at the distance of 7cm from the coil center. Because of using slidac, the rotation frequency of the micromotor is fixed at 60Hz. It has already shown in section 4.2 that in a magnitude of 0.03mT, the permanent magnet rotates stably when the frequency range of the external magnetic field is between 25-115Hz. The present system can promote a smooth rotation of the permanent magnet and the suitable distance.

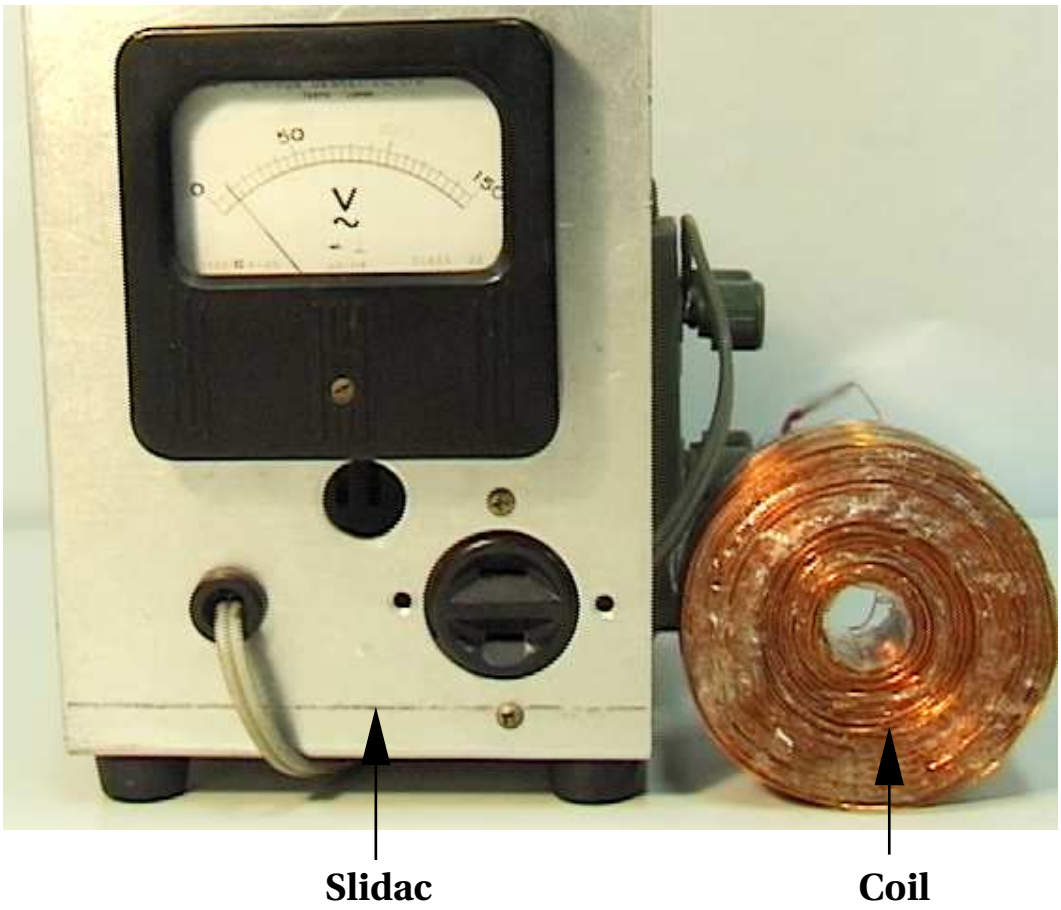

Figure 4.1. Generation of external magnetic field

4.2. Signal acquisition system

Fig.4.2 illustrates the block diagram of the signal acquisition system. The catheter is inserted into the object and placed into a water tub. The rotation of the micromotor is controlled by the external magnetic field generated from a coil and the coil is connected with a slidac. In present system, the micromotor rotation frequency(MRF) is set at 60rps and the pulse repetition frequency(PRF) of ultrasound beam is set at 10kHz.

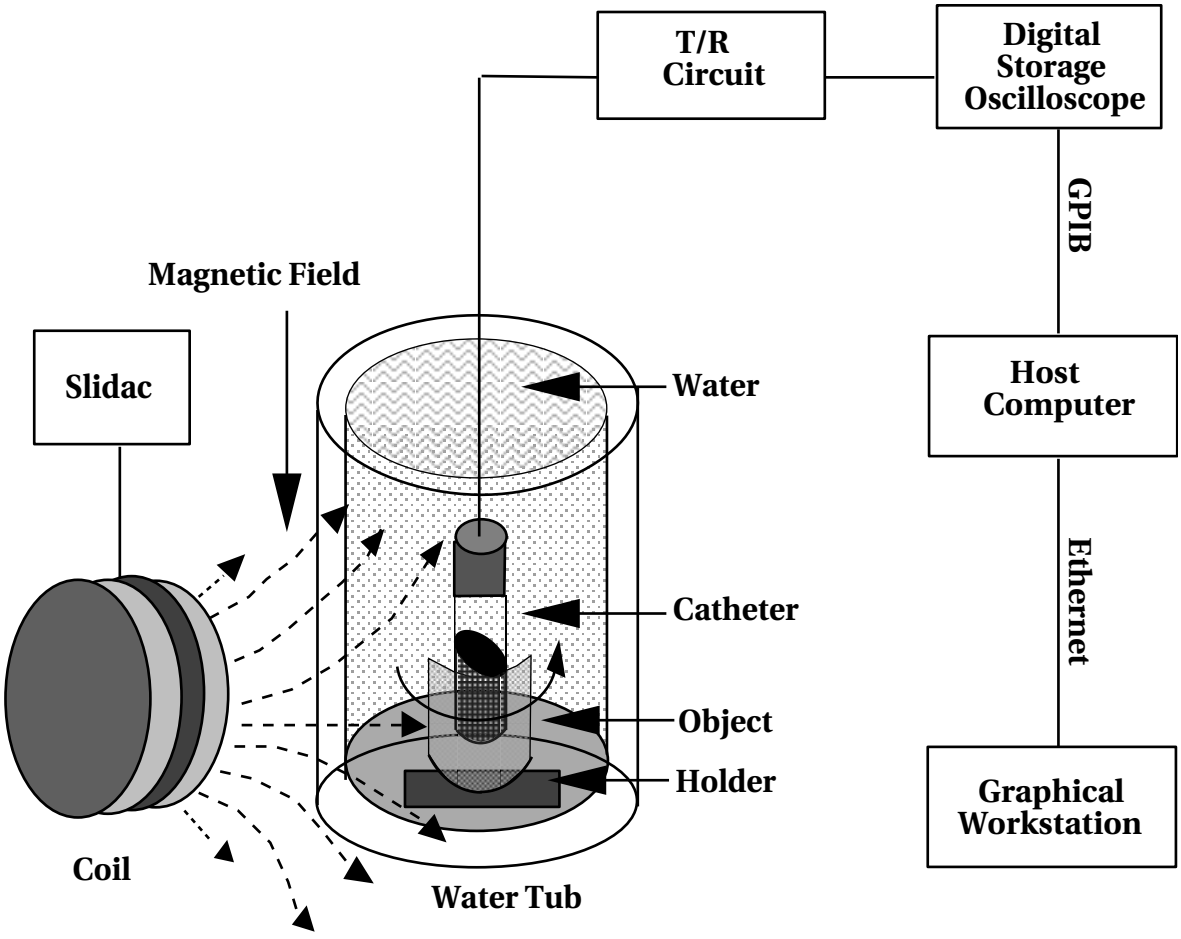

Figure 4.2. Block diagram of the data acquisition system

Inside the catheter, ultrasound beam from the transducer having a resonant frequency of 20MHz is reflected by the mirror and transmitted towards the object. Echo signals from the object are reflected by the mirror and received by the same transducer. The sequencing of ultrasound beam transmission/reception is performed and controlled by the T/R circuit. The echo signals are amplified 20 times and stored in a digital storage oscilloscope (LeCroy 9354L) at a sampling rate of 250MHz. Fig.4.3(a) shows a photograph of the digital storage oscilloscope. The stored data are then transferred to a host computer (Sun SPARC Station 2) through GPIB. Fig.4.3(b) shows a photograph of the host computer.

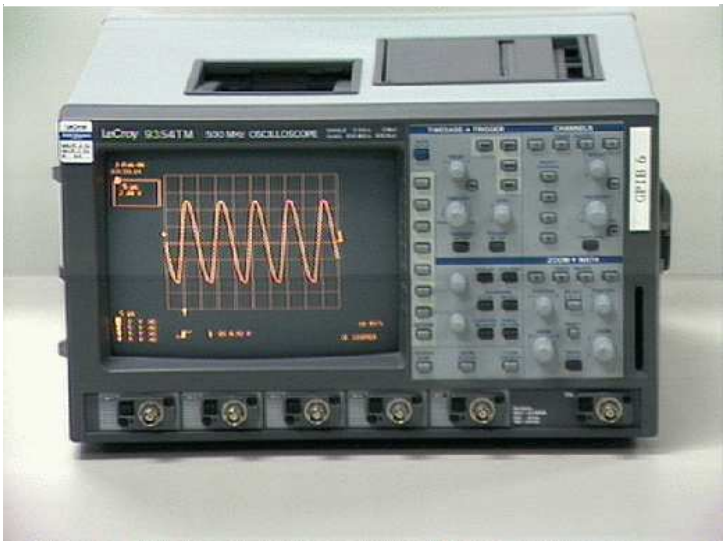

LeCroy 9354L

(a)

Sun SPARC Station 2

(b)

Figure 4.3. Signal acquisition system, (a)Digital storage oscilloscope, (b)Host computer

To enhance the S/N ratio, the received data are filtered by a Bessel band-pass filter between 17−23.5MHz on the host computer. Fig.4.4 shows the frequency response of a band-pass Bessel filter.

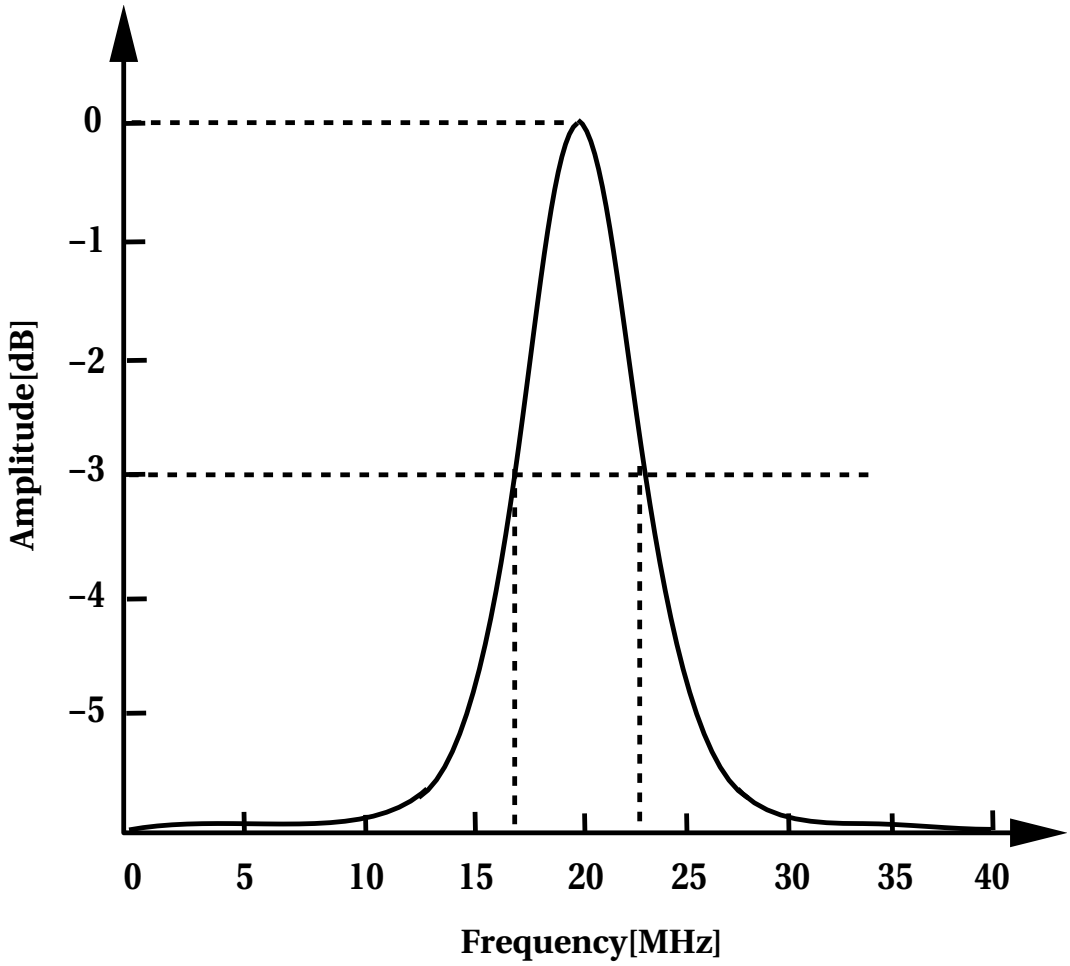

Figure 4.4. Frequency response of a Bessel band-pass filter

4.3. Image reconstruction process

The number of scan lines, NSL, to reconstruct a cross-sectional image was set to 167 according to eq.(4.1),

$$NSL = PRF/MRF, \tag{4.1}$$

The filtered data from the host computer are transferred to a graphical workstation (SGI Indigo^2) through ethernet where the cross-sectional image of the object is reconstructed. Fig.4.5 shows a photograph of the graphical workstation.

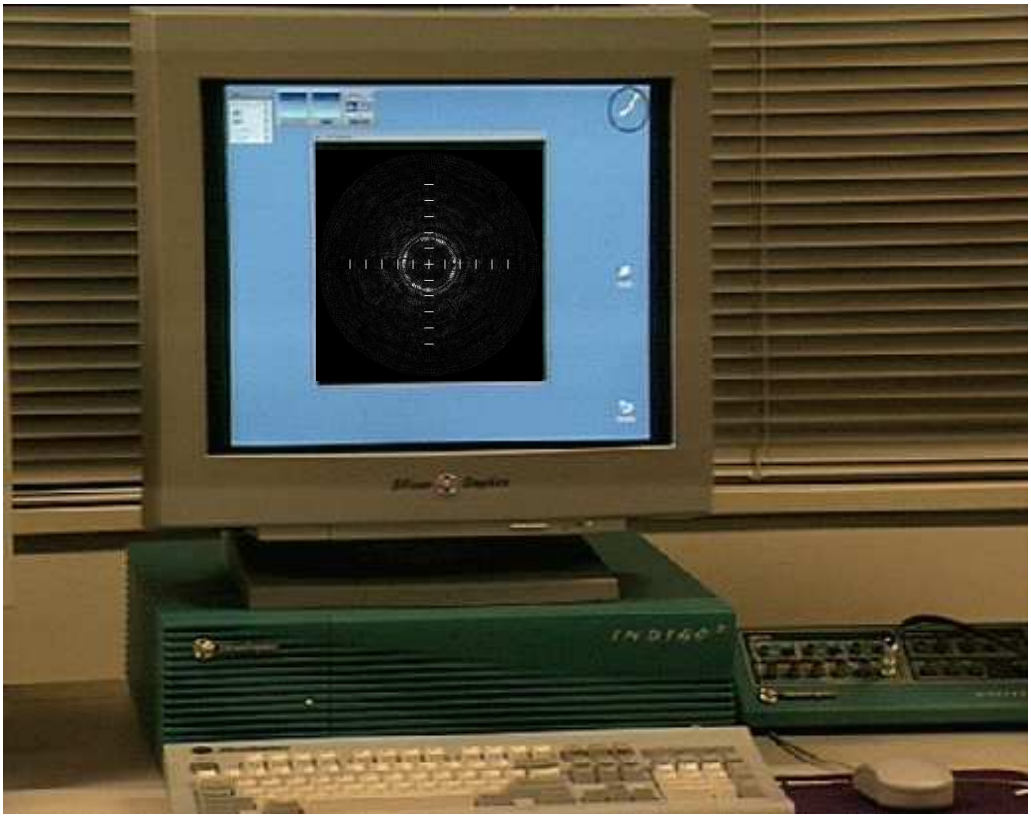

Figure 4.5. Graphical workstation

In the image reconstruction process, first, the absolute value of the echo signals from 167 scan lines are calculated. Second, the absolute values are quantized to a 8-bit gray scale level. Finally, the gray scale data of each scan line are plotted radially in order of their receiving time as shown in fig.4.6. The gap between scan lines are filled with a linear interpolation.

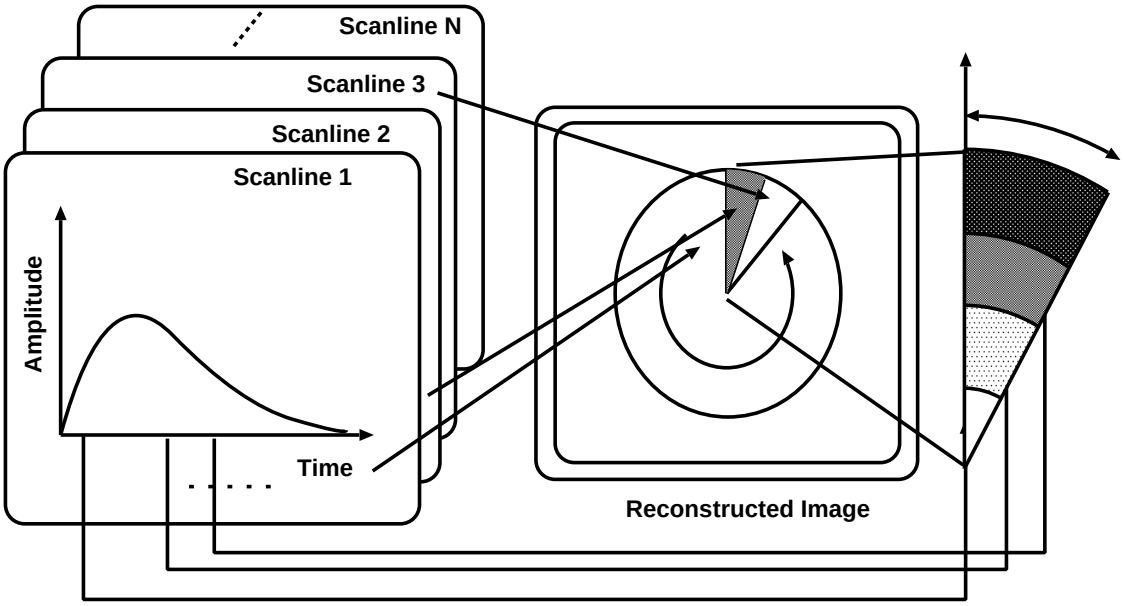

Figure 4.6. Image reconstruction process

Chapter 5

Experiments and Results

5.1. Phantom experiments

The objective of phantom experiments was to evaluate the measurement accuracy of the present micromotor type IVUS endoscope. Three different types of phantoms were prepared for this purpose. The phantoms were set in a water tub and the catheter was fixed inside the phantom as shown in fig.5.1 and the cross-sectional images were reconstructed from the acquired echo-data.

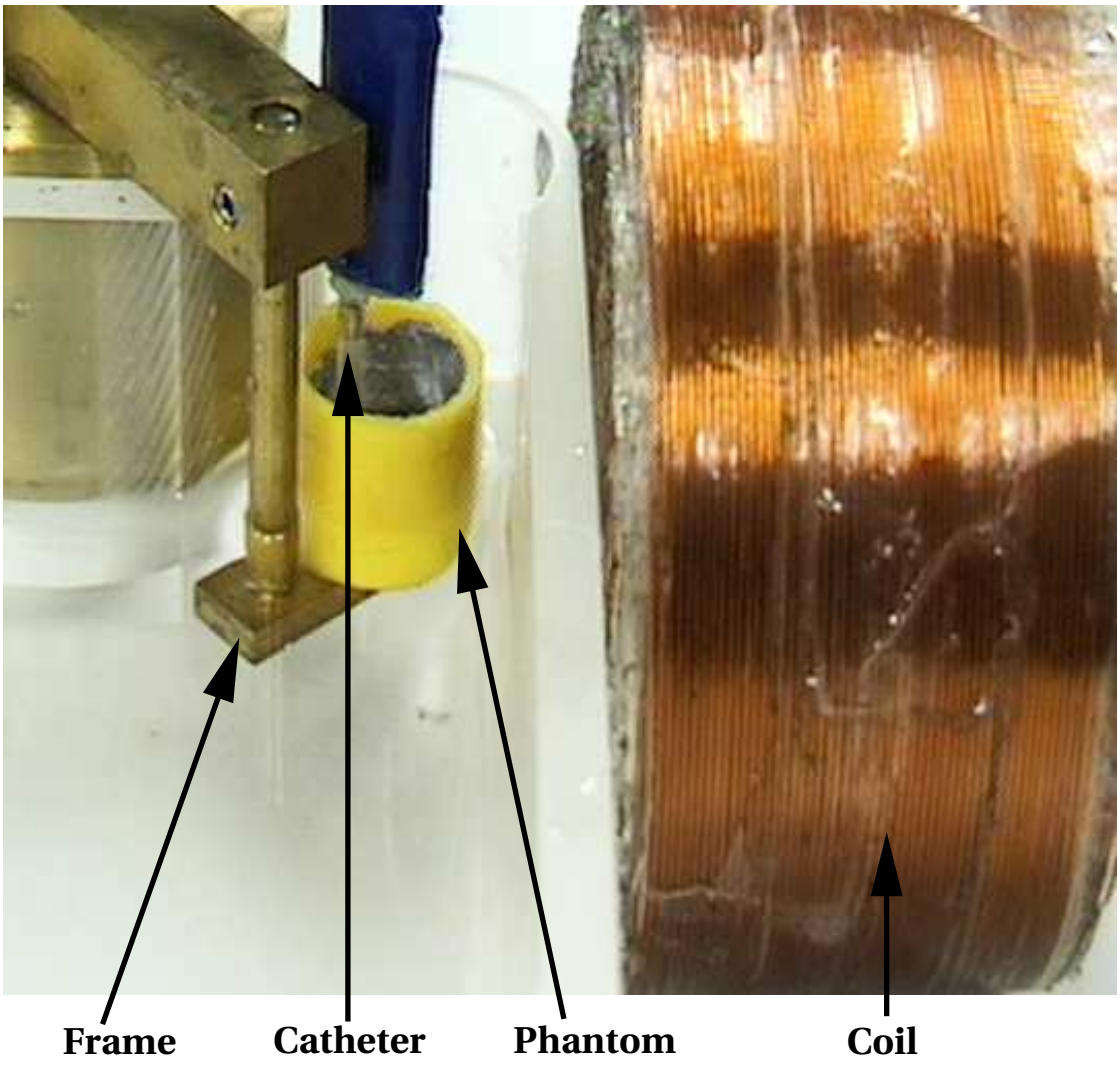

Figure 5.1. A view of phantom experiment

- Phantom 1

  Fig.5.2 shows a photograph of phantom1. Phantom1 is a cylinder shaped plastic tube having an inner diameter of 8mm and a outer diameter of 10mm. Inside the tube, a thin paper of Al was pasted.

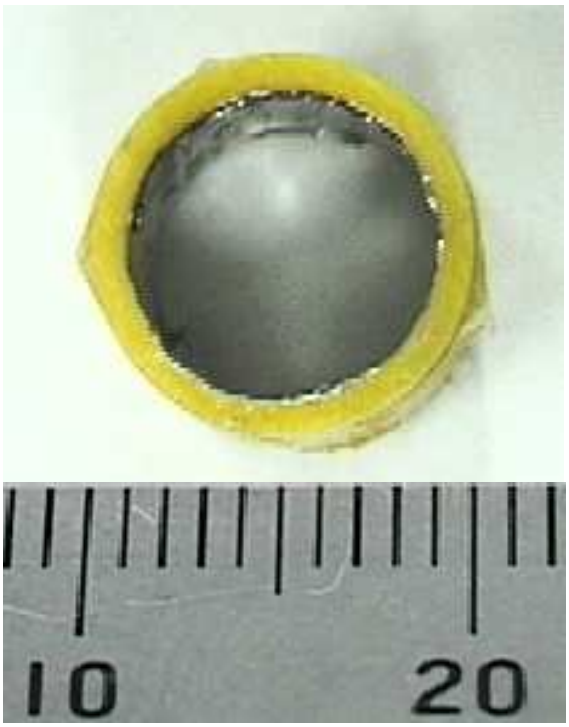

Figure 5.2. A photograph of phantom1

Fig.5.3(a) shows an example of the echo signal waveform. In this echo signal, the first peak corresponds to the echo from the catheter tube and the second peak to the echo from the phantom wall.

Fig.5.3(b) shows the reconstructed image of phantom1. The scale in the image is 2.5mm/div. Here the cross-section of the tube is reconstructed at the distance of 8-11mm from the center. The average thickness of the phantom1 wall is measured 1.1mm. The catheter tube is also reconstructed at the origin of reconstructed image.

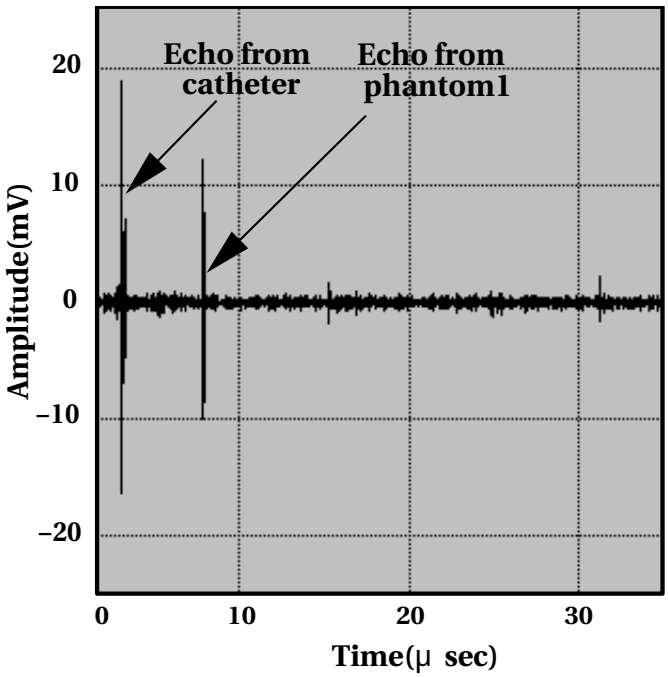

(a)

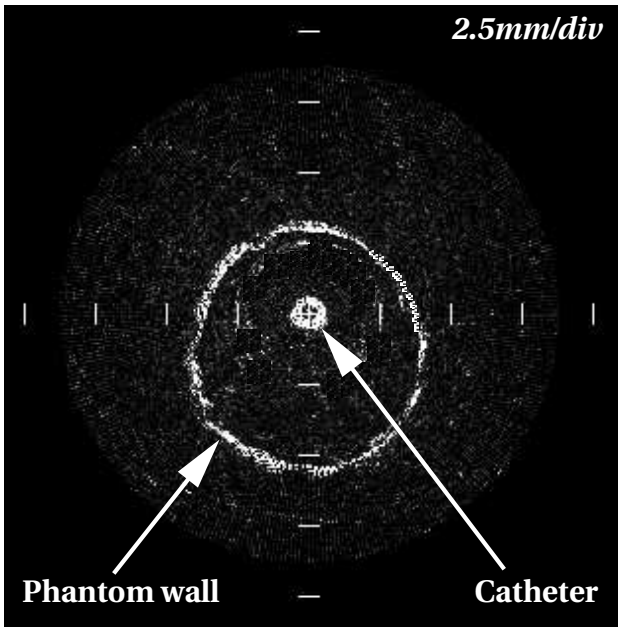

(b)

Figure 5.3. Results of phantom1, (a)an echo signal, (b)reconstructed image.

- Phantom 2

  Fig.5.4 shows a photograph of phantom2. Phantom2 is a half-circled cylinder shaped plastic tube having an inner diameter of 8mm and a outer diameter of 10mm. Inside of the tube, a thin paper of Al was pasted.

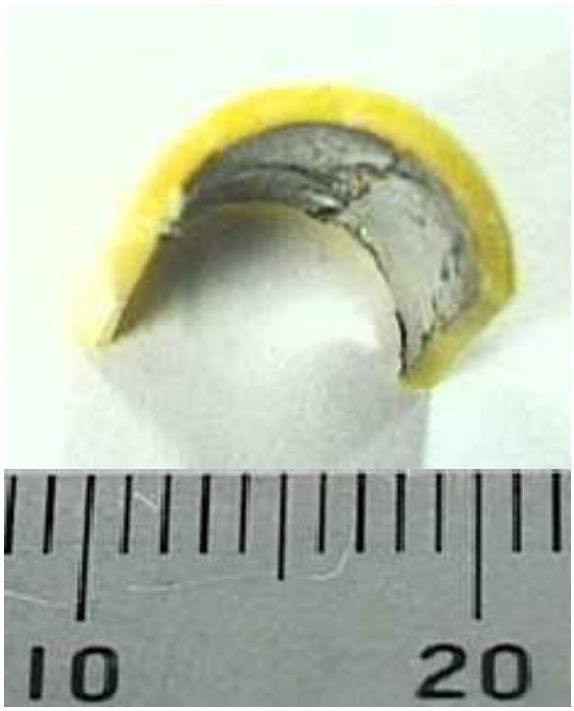

Figure 5.4. A photograph of phantom2

Fig.5.5(a) shows an example of the echo signal waveform. In this echo signal, the first peak corresponds to the echo from the catheter tube and the second peak to the echo from the phantom wall.

Fig.5.5(b) shows the reconstructed image of phantom2. The scale in the image is 2.5mm/div. Here the cross-section of the tube is reconstructed at the distance of 8-11mm from the center. The average thickness of the phantom2 wall is measured 1.1mm. The catheter tube is also reconstructed at the origin of reconstructed image.

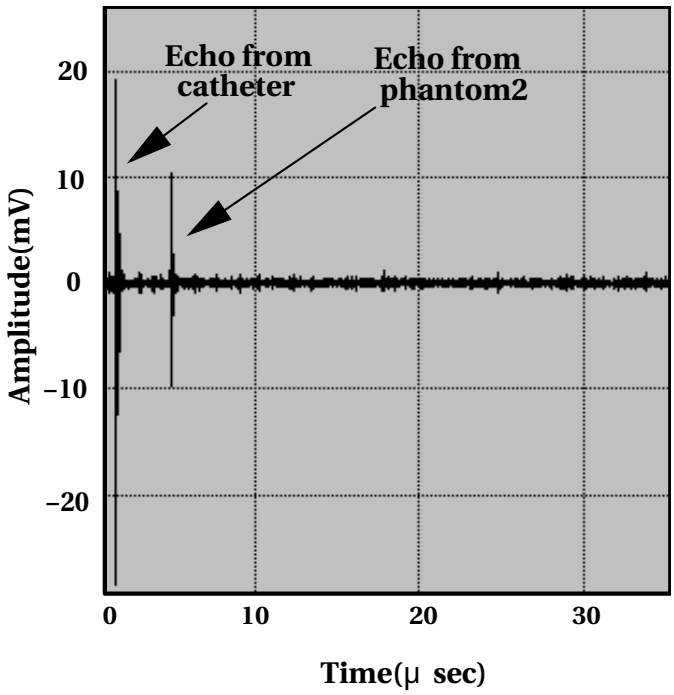

(a)

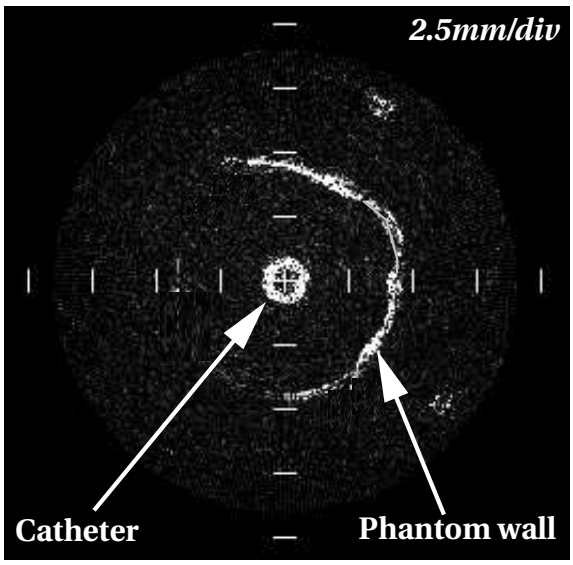

(b)

Figure 5.5. Results of phantom2, (a)an echo signal, (b)reconstructed image.

- Phantom 3

  Fig.5.6 shows a photograph of phantom3. Phantom3 is a cylinder shaped plastic tube with the same size as phantom1, where a material made with Ca and wax of candle is set as a simulation of stricture.

Figure 5.6. A photograph of phantom3

Fig.5.7(a) shows an example of the echo signal waveform. In this echo signal, the first peak corresponds to the echo from the catheter tube, the second peak to the echo from the stricture and the third peak to the echo from the phantom wall.

Fig.5.7(b) shows the reconstructed image of phantom3. The scale in the image is 2.5mm/div. Here the cross-section of the tube is reconstructed at the distance of 8-11mm from the center and the stricture part is reconstructed at the distance of 6-8mm from the center. The average thickness of the phantom3 wall is measured 1.1mm and the stricture is 2mm. The catheter tube is also reconstructed at the origin of the reconstructed image.

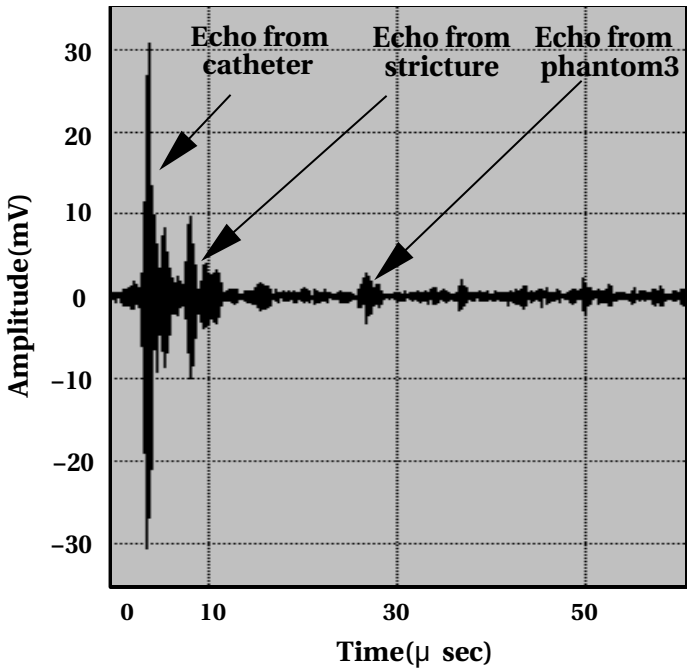

(a)

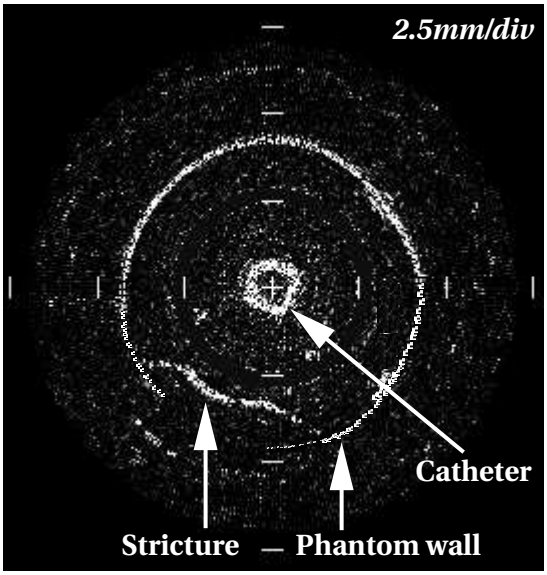

(b)

Figure 5.7. Results of phantom3, (a)an echo signal, (b)reconstructed image.

5.2. In vitro experiments

In vitro experiments were carried on two human arterial specimens to visualize the arterial walls. The arterial specimens were mounted on the frame in the water tub as shown in fig.5.8 and then the catheter was inserted into the arterial specimens for imaging. Finally, the images were reconstructed.

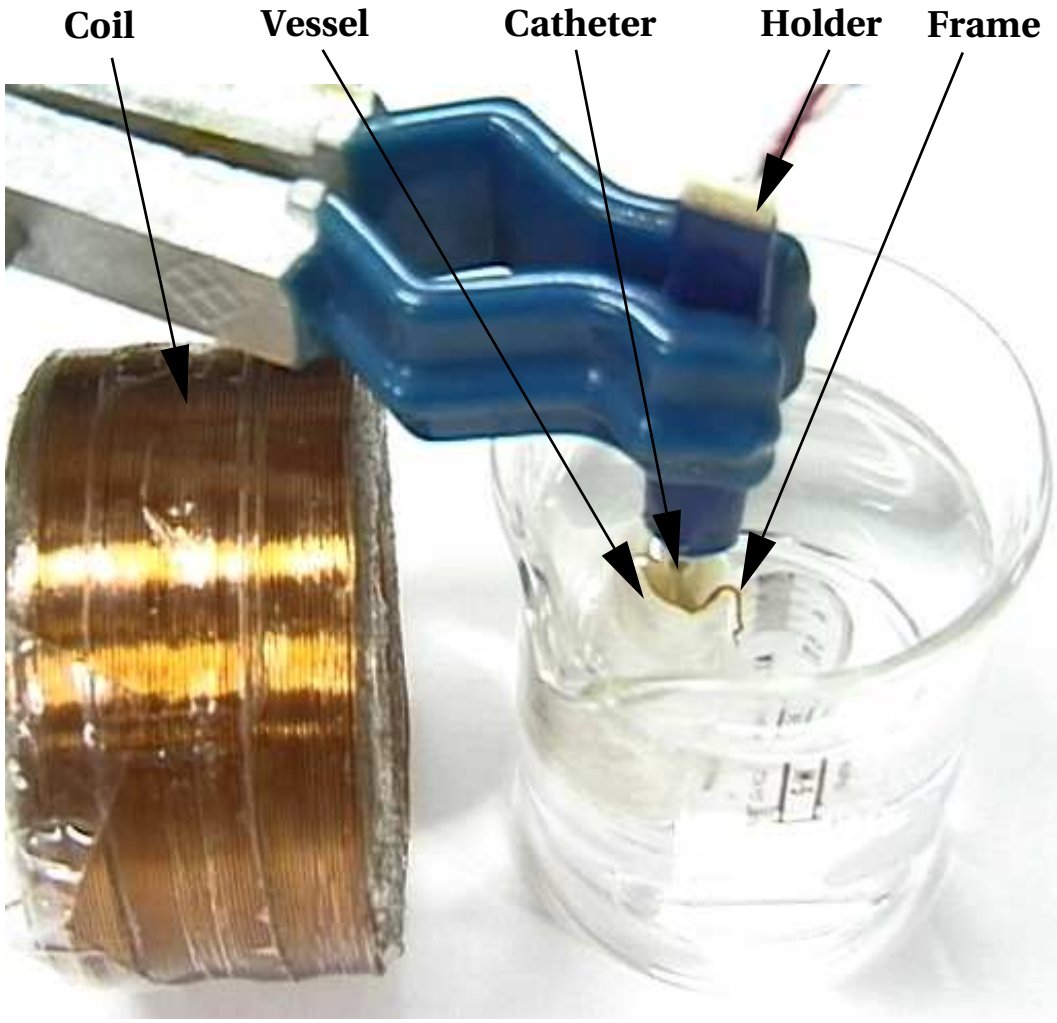

Figure 5.8. A view of in vitro experiment

- Specimen1
  Fig.5.9 shows a photograph of arterial specimen1.

Figure 5.9. A photograph of arterial specimen1

Fig.5.10(a) shows an example of the echo signal waveform from the arterial wall. In this echo signal, the first peak corresponds to the echo from the catheter tube and the second peak to the echo from the arterial wall.

Fig.5.10(b) shows the reconstructed image of arterial specimen1. The scale in the image is 2.5mm/div. Here the cross-sectional image of the artery is reconstructed at the distance of 8-10mm from the center. The average thickness of the arterial wall is measured 1.25mm. The catheter tube is also reconstructed at the origin of the reconstructed image.

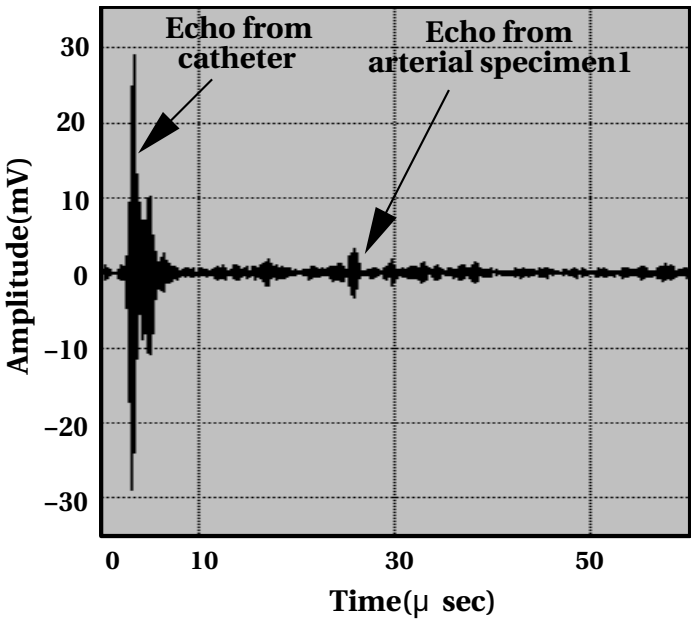

(a)

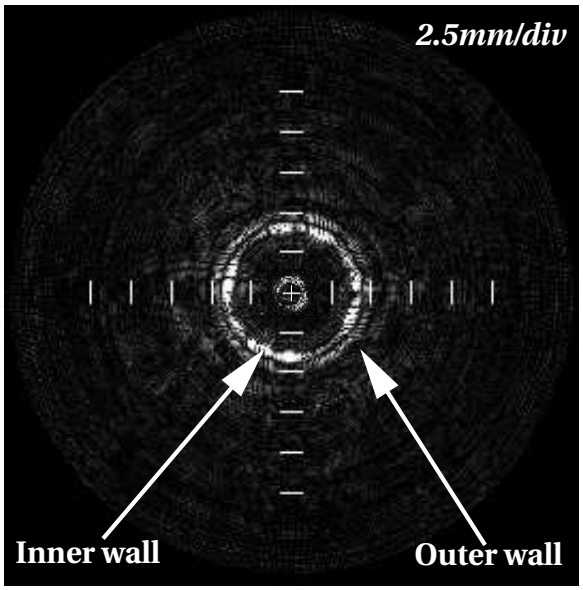

(b)

Figure 5.10. Results of arterial specimen1, (a)example of an echo signal, (b)cross-sectional image of arterial specimen1.

- Specimen2
  Fig.5.11 shows a photograph of arterial specimen2.

Figure 5.11. A photograph of arterial specimen2

Fig.5.12(a) shows an example of the echo signal waveform from the arterial wall. In this echo signal, the first peak corresponds to the echo from the catheter tube and the second peak to the echo from the arterial wall.

Fig.5.12(b) shows the reconstructed image of arterial specimen2. The scale in the image is 2.5mm/div. Here the cross-sectional image of the artery is reconstructed at the distance of 4-7mm from the center. The average thickness of the arterial wall is measured 1.45mm. The catheter is also reconstructed at the origin of the reconstructed image.

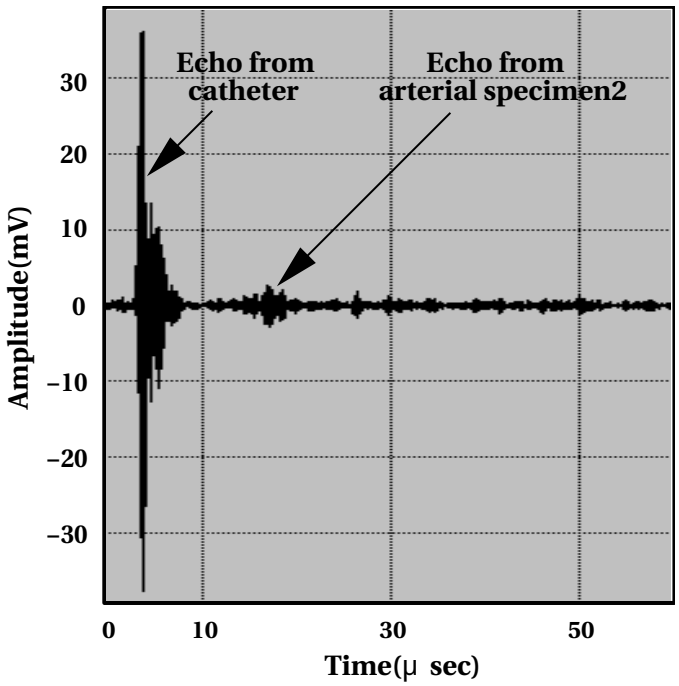

(a)

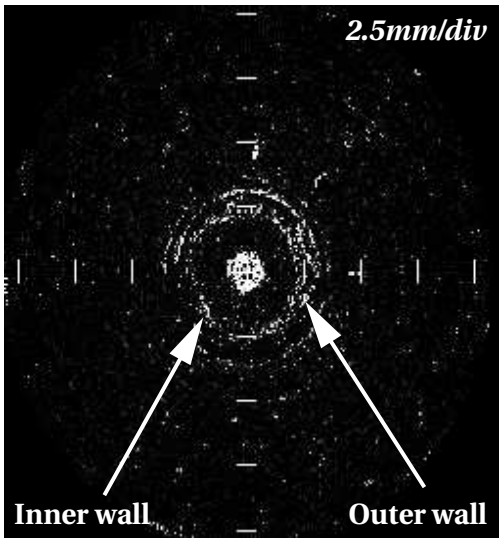

(b)

Figure 5.12. Results of arterial specimen2, (a)example of an echo signal, (b)cross-sectional image of arterial specimen2.

Chapter 6

Discussion

The phantom experiment results show a suitable correlation between the acquired diameter and shape of the phantom with its actual diameter and shape. These results proved that the present system has sufficient accuracy of measuring the luminal diameter. However, in the reconstructed images, the outer wall of the phantom was blurred and not clear enough in some part. It was due to the attenuation of ultrasound at the outer wall and the re-reflects from the phantom. Furthermore, there was a slight overestimation of 10% in the wall thickness derived by the micromotor type IVUS. This overestimation is caused by the spread-out characteristics of ultrasound beam. The distance between the transducer center and the border of near-field and far-field, DNF, can be calculated with eq.(6.1),

$$DNF = D^2/4\lambda, \tag{6.1}$$

where D is the diameter of transducer and λ is the wavelength. In present system, D is 12mm and λ is 0.075mm. The distance between the transducer center and the border of near-field and far-field is 4.8mm. From this point, ultrasound beam starts to spread out at the catheter tube and it results in some unexpected echo signals, for example, echo signals from the surface of the shaft on which the micromotor was set for the smooth rotation. This spread out characteristics of ultrasound is also attributed to differences of resolution in the interest area. To solve this problem, a recent study was carried out by Furuya et al. on several IVUS images of a canine carotid using a two-dimensional range-variant Gaussian shaped inverse filter[23]. The experiment results of Furuya et al. revealed that the

spread out of ultrasound beam can be suppressed, and a high resolution can be preserved on the entire interest area using this two-dimensional inverse filter. This two-dimensional range-variant Gaussian shaped inverse filter can be applicable to present micromotor type IVUS endoscope for reducing the unexpected echo data due to the spread out characteristics of ultrasound.

In the in vitro experiment results, the echo signal from the catheter tube was large comparing with the echo signal from the arterial wall. Here, I emphasized the echo signals from the arterial wall to visualize the arterial specimens clearly. The result of in vitro experiments show that the present system has sufficient ability to visualize the arterial wall and to measure the thickness. However, in the reconstructed images, the edge of the both inner and outer walls were distorted and not clear enough. It was due to the insufficient S/N ratio of present measurement system and the low resonant frequency of present ultrasound transducer. To enhance the S/N ratio, a low noise amplifier is needed to be set in our present measurement system. The micromotor type IVUS endoscope of present system using a 20MHz frequency transducer does not provide a high resolution. When a higher frequency IVUS transducer of 40−50MHz is now available, the resolution may be increased.

The catheter size of micromotor type IVUS endoscope is small enough to visualize a cross-sectional image of artery. Furthermore, a micromotor type IVUS can be made smaller for observation of coronary vessels because of its simple design. This simplicity, in addition, enables one to implement other functions with the catheter.

Conclusions

I developed a new lateral-viewing micromotor type IVUS endoscope. To evaluate the measurement accuracy of this micromotor type IVUS endoscope, I performed several phantom experiments and applied this to observe the inside of human arterial specimens through in vitro experiments. The reconstructed images demonstrated that the lateral-viewing micromotor type IVUS endoscope had the potential to visualize the arterial wall accurately. Furthermore, it could measure the arterial wall thickness to diagnose diseases like blood vessel stricture, vessel lesion, etc.

These preliminary experiment results were very encouraging. These results suggested that this technique is promising for an IVUS endoscope and that it can solve the rotation transmitting wire problem of conventional IVUS endoscope. My research on lateral-viewing micromotor type IVUS endoscope is in the preliminary stage now and in future, it is needed to proceed in vivo experiments to evaluate the ability of this system in practical uses for a clinical purpose.

Acknowledgements

I am grateful to many people for their valuable assistance to my research work. I would like to thank my supervisor Professor Kunihiro Chihara of Graduate School of Information Science for his valuable comments and support to my research work.

Thanks also to my second supervisor Professor Kyohiro Shikano of Graduate School of Information Science for his assistance on this thesis and helpful suggestions.

Special thanks to Associate Professor Osamu Oshiro of Research Center for Advanced Science and Technology and Research Associate Ayumu Matani of Graduate School of Information Science for their technical guidance and valuable advice to my research work. All of this work would not have been possible without their help with the Japanese language and with the difficulties concerning my study in Japan.

I am also very grateful to Professor Masato Asao of Osaka National Hospital, Akitosi Itou of Zeon Medical Ltd. and Keiichi Murakami of Fujitsu Co. Ltd. for providing me all the necessary materials required in present study.

I should also thank to Associate Professor Kosuke Sato of Graduate School of Information Science and Research Associate Qian Chen of Graduate School of Information Science for their valuable suggestions to my research work.

Last but not least I am very grateful to secretary Nobuko Ui and all the students of Image Processing Laboratory of Graduate School of Information Science for their active support and help to me in overcoming the barrier of Japanese language and other difficulties concerning my life in Japan.

References

[1] T. Wagai and N. Kousi: Basis of Ultrasound Diagnostic System and Technology(in Japanese). Vector Core, 1994.

[2] R. N. Thurston and A. D. Pierce: Ultrasonic Measurement Methods. Academic Press, Vol.XIX, 1990.

[3] K. T. Dussik: Uber die moglichkeit, hoch frequente mechanische schwingungen als diagnostisches heifsmittel zu verwenden. Z. Neurol., Vol.174, p.153, 1942.

[4] K. T. Dussik: Ultraschallanwending in der diagnostik and therapie der erkrankungendes zentralen newensystems. Ultraschall in Der Medizin, p.283, 1949.

[5] J. J. Wild and J. M. Reid: The effect of biological tissues on 15-Mac pulsed ultrasound. J. Acoust. Soc. Am., Vol.25, p.270, 1953.

[6] F. S. Foster, C. J. Pavlin, G. R. Lockwood, L. K. Ryan, K. A. Karasiewicz, L. Berube and A. M. Rasuth: Principle and applications of ultrasound backscatter microscopy. IEEE Transactions on Ultrasonic. Ferroelectric and Frequency Control, Vol.40, No.5, p.608, 1993.

[7] S. Webb: The Physics of Medical Imaging. Adam Hilger, 1988.

[8] W. J. Gussenhoven, C. E. Essed, P. Frietman, F. Mastik, C. Lancee, C. Slager, P. Serruys, P. Gerritsen, H. Pieterman and N. Bom: Intravascular echographic assessment of vessel wall characteristics: a correlation with histology. Intl. J. of Cardiac Imaging, Vol.4, pp.105-116, 1983.

[9] E. J. Gussenhoven, C. E. Essed, C. T. Lancee, F. Mastik, P. Frietmen, F. C. Vanegmond, J. Reiber, H. Bosch, H. Vanurk, J. Roelandt and N. Bom: Arterial wall characteristics determined by intravascular ultrasound imaging: an in vitro study. J. of Am. Coll. Cardiology. Vol.14, No.4, pp.947-952, 1989.

[10] J. A. Mallery, J. M. Tobis, J. Griffith, J. Gessert, M. McRae, O. Moussabeck, M. Besen, M. Moriuchi and W. L. Henry: Assessment of normal and atherosclerosis arterial wall thickness with an intravascular ultrasound imaging catheter. Am. Heart J., Vol.119, pp.1392-1400, 1990.

[11] W. F. Ganong: Review of Medical Physiology. Appleton & Lange, 1991.

[12] D. M. Cavaye, M. R. Tabbara, G. E. Kopchok, T. E. Laas and R. A. White: Three dimensional vascular ultrasound imaging. J. of Am. Surgeon, Vol.12, pp.751-755, 1991.

[13] G. E. Kopchok, R. A. White and C. Guthrie: Preliminary report of dimensional and morphologic accuracy. Ann Vsc Surg, Vol.4, pp.291-296, 1990.

[14] K. Yamamoto, M. Shikutani, T. Amano and E. Okamoto: An intravascular ultrasonic imaging technique for measurement of elastic properties of the artery. Acoustical Imaging, Vol.20, pp.433-440, 1993.

[15] Md. Salimuzzaman, A. Matani, O. Oshiro, K. Chihara, M. Asao and T. Furukawa: 3D Reconstruction of intravascular ultrasonic images using a micromotor(in Japanese). Proceedings of the 35th Conference of Japan Society of Medical Electronics and Biological Engineerings, Vol.34, p.223, 1996.

[16] Md. Salimuzzaman, A. Matani, O. Oshiro, K. Chihara and M. Asao: Visualization of a blood vessel using a micromotor. Technical Digest of 14th Sensor Symposium, I.E.E. of Japan, pp.279-280, 1996.

[17] Z. H. Cho, J. P. Jones and M. Singh: Foundation of Medical Imaging. Wiley-Interscience, 1993.

[18] K. K. Shung, M. B. Smith and B. Tsui: Principles of Medical Imaging. Academic Press, 1992.

[19] N. Fujita, K. Mijusige and H. Matsuo: The present condition of intravascular ultrasound(in Japanese). A Monthly Journal of Medical Imaging and Information, Vol.26, No.12, p.662, 1994.

[20] Md. Salimuzzaman, A. Matani, O. Oshiro, K. Chihara and M. Asao: Blood vessel visualization using a micromotor IVUS (in Japanese). Proceedings of the Electronics, Information and Systems Conference, I.E.E. of Japan, pp.141-142, 1996.

[21] S. Matsumoto, O. Oshiro, K. Chihara, A. Iida, K. Kawabe, T. Shimura, M. Asao and T. Furukawa: Intravascular ultrasonic imaging with a micromotor. Jpn. J. Appl. Phys., Vol.34, pp.2865-2868, 1995.

[22] Md. Salimuzzaman, A. Matani, O. Oshiro, K. Chihara and M. Asao: A micromotor for blood vessel visualization(in Japanese). The 17th Symposium on Ultrasonic Electronics, p.155, 1996.

[23] N. Furuya, S. Yagi, M. Nishimura and K. Ogawa: 2-Dimensional range-variant inverse filtering to intra-vascular ultrasound image(in Japanese). Basic Technology, The Japan Society of Ultrasonics in Medicine, Vol.96, No.4, pp.19-25, 1997.